Journal of Pharmaceutical Sciences 111 (2022) 175–184

Contents lists available at ScienceDirect

Journal of Pharmaceutical Sciences

journal homepage: www.jpharmsci.org

Pharmaceutics, Drug Delivery and Pharmaceutical Technology

Comparison of Cellular Monolayers and an Artificial Membrane as Absorptive Membranes in the *in vitro* Lipolysis-permeation Assay

Janneke Keemink[a,b], Oliver J. Hedge[a], Valentina Bianco[a], Madlen Hubert[a], Christel A.S. Bergström[a,c,*]

[a] *Department of Pharmacy, Uppsala University, Uppsala, Sweden*
[b] *F. Hoffmann-La Roche Ltd., Basel, Switzerland*
[c] *The Swedish Drug Delivery Center, Department of Pharmacy, Uppsala University, Uppsala, Sweden*

ARTICLE INFO

Article history:
Received 14 July 2021
Revised 7 September 2021
Accepted 7 September 2021
Available online 10 September 2021

Keywords:
Lipid-based formulation(s)
Self-emulsifying
In vitro model(s)
Light scattering (dynamic)
Oral absorption
Disposition
Caco-2 cells
MDCK cells
Passive diffusion
Biomimetic(s)

ABSTRACT

Permeation across Caco-2 cells in lipolysis-permeation setups can predict the rank order of *in vivo* drug exposure obtained with lipid-based formulations (LBFs). However, Caco-2 cells require a long differentiation period and do not capture all characteristics of the human small intestine. We therefore evaluated two *in vitro* assays with artificial lecithin-in-dodecane (LiDo) membranes and MDCK cells as absorptive membranes in the lipolysis-permeation setup. Fenofibrate-loaded LBFs were used and the results from the two assays compared to literature plasma concentrations in landrace pigs administered orally with the same formulations. Aqueous drug concentrations, supersaturation, and precipitation were determined in the digestion chamber and drug permeation in the receiver chamber. Auxiliary *in vitro* parameters were assessed, such as permeation of the taurocholate, present in the simulated intestinal fluid used in the assay, and size of colloidal structures in the digestion medium over time. The LiDo membrane gave a similar drug distribution as the Caco-2 cells and accurately reproduced the equivalent rank-order of fenofibrate exposure in plasma. Permeation of fenofibrate across MDCK monolayers did not, however, reflect the *in vivo* exposure rankings. Taurocholate flux was negligible through either membrane. This process was therefore not considered to significantly affect the *in vitro* distribution of fenofibrate. We conclude that the artificial LiDo membrane is a promising tool for lipolysis–permeation assays to evaluate LBF performance.

Introduction

A persistent problem for the pharmaceutical industry is poor aqueous solubility of promising drug candidates and thus the large proportion of new drugs are poorly soluble in gastrointestinal (GI) fluids. Poor solubility often leads to insufficient and erratic oral absorption.[1,2] Oral drug products based on lipid-based formulation (LBF) technology—such as self-emulsifying drug delivery systems—typically enhance the solubility of lipophilic compounds in the GI tract, making them valuable tools for improving the solubility-limited oral bioavailability of these compounds.[3,4] However, market penetration of LBFs is limited in part because bioavailability is difficult to predict with current *in silico* and *in vitro* tools.[2,5] Until recently, predictions have typically involved digestion of LBFs during *in vitro* lipolysis experiments. These measure the rate and extent of lipid digestion and the impact of this process on aqueous drug concentrations in biorelevant media.[6] Unfortunately, this methodology seldom results in physiologically accurate predictions,[7,8] meaning expensive and time-consuming empirical animal experiments are required to confirm *in vivo* exposure.[4]

In the small intestine, drugs are absorbed during digestion and solubilization. Since the complex interplay between the intraluminal processes of digestion, solubilization and absorption is not captured by the *in vitro* lipolysis assay, it has been proposed to include an absorption compartment to improve predictions.[4] Absorption has been introduced by: (i) coupling *in vitro* lipolysis to *in situ* animal absorption,[9] (ii) performing consecutive lipolysis and permeation experiments,[10–13] or (iii) applying biopharmaceutical *in silico* modeling to account for the absorption sink.[14]

We recently introduced the first full *in vitro* lipolysis-permeation setup that simultaneously evaluates the intraluminal processes. The

Abbreviations: LBFs, Lipid-Based Formulation; GI, gastrointestinal; LC, Long-Chain; MC, Medium-Chain; LiDo, Lecithin-in-Dodecane; PVDF, Polyvinylidene Difluoride; BSA, Bovine Serum Albumin; SDS, Sodium Dodecyl Sulfate; FaSSIF, Fasted State Simulated Intestinal Fluid; PBS, Phosphate Buffered Saline; AUC, Area Under the Curve; IVIVR, *In Vitro In Vivo* Relationship; MDCK, Madin-Darby Canine Kidney.

* Corresponding author at: Department of Pharmacy, Husargatan 3, Box 580, SE-75123 Uppsala, Sweden.
E-mail address: christel.bergstrom@farmaci.uu.se (C.A.S. Bergström).

https://doi.org/10.1016/j.xphs.2021.09.009

setup consists of two compartments: an upper chamber for digestion and a lower one for absorption, separated by a Caco-2 cell monolayer.[15,16] With this experimental setup, drug transfer across the Caco-2 cells to the receiver compartment (absorption chamber) accurately predicted plasma exposure rank-order for: (i) three LBFs loaded with fenofibrate, administered to landrace pigs,[15] and (ii) carvedilol predissolved in or co-administered with LBF, administered to Labrador dogs.[17] The dissolved drug in the donor compartment (digestion chamber) did not accurately predict the plasma exposure ranking; however, the rate and extent of digestion could be followed while the drug permeated into the receiver chamber.

Despite the harsh digestive conditions, a well-stirred compartment and the use of lipase immobilized on polymeric beads allowed the use of Caco-2 cell membranes. While Caco-2 cells are considered the gold standard for oral absorption studies, they typically demand 21 days to differentiate and maintenance every 2–3 days.[18] Furthermore, paracellular diffusion across the monolayer is limited, due to the narrow pore size of the tight junctions in this colon-derived cell model. We therefore evaluated the use of alternative absorptive membranes and selected Madin-Darby canine kidney (MDCK) cells. Although of kidney origin, this model is extensively used to estimate intestinal permeation during drug discovery as it produces suitable monolayers within four days.[19,20] These cells also form larger paracellular pores than Caco-2 cells.[19] A second membrane, a generic artificial membrane (LiDo), analogous to the commercially available GIT-0 lipid membrane, was selected due to its ability to withstand the digestion medium.[5] We then compared the *in vivo* relevance of the data obtained with Caco-2, MDCK and LiDo membranes in the lipolysis-permeation setup, with literature data of drug absorption in landrace pigs after administration of various LBFs.[21]

Additionally, lipid digestion and bile salt permeation may affect the colloidal structures in the donor media, which in turn might affect the solubilization capacity of the donor media as well as the absorption rate of a loaded drug.[22] We therefore also measured the size of colloidal structures during digestion and taurocholate permeation across the absorptive membranes.

Materials and Methods

Materials

Acetonitrile (≥ 99.9%), 4-bromophenol boronic acid, bovine serum albumin (BSA), carbitol (diethylene glycol monoethyl ether), D-α-tocopherol polyethylene glycol succinate (TPGS), dimethyl sulfoxide (DMSO ≥ 99.9%), fenofibrate, fenofibric acid, Hanks' Balanced Salts (HBSS, without phenol red and sodium bicarbonate), Kolliphor RH40 (macrogolglycerol hydroxystearate), lecithin extract (Avanti's "Soy PC (20%)"), methanol (99.9%), olive oil, taurocholate, Tris-maleate, Tween 85, and warfarin were purchased from Merck (Darmstadt, Germany). Novozyme 435 (immobilized lipase) was obtained from Strem Chemicals (Bischheim, France). Miglyol 812 N was obtained from IOI Oleo (Wittenberge, Germany). FaSSIF/FeSSIF/FaSSGF powder was bought from Biorelevant.com (Croydon, UK). Lucifer Yellow CH dilithium salt was obtained from Biotium (Fremont, CA, USA). *N*-dodecane (≥ 99%) was obtained from Alfa Aesar (Lancashire, UK). Ethanol (99.5%, denatured with 0.4% isopropyl alcohol) was obtained from Solveco (Rosersberg, Sweden). All water used was of grade I from a Milli-Q water purification system (Merck).

Lipid-based Formulations (LBFs)

Formulations were selected for this study (Table 1) based on their previous usage.[5,15,21] They are representative of different classes according to the Lipid Formulation Classification System (LFCS),[23] as IIIA-MC, IIIA-LC and IV. The LFCS categorizes oral LBFs in five categories (I, II, IIIA, IIIB, and IV) based on the composition. Type I formulations are pure lipid compositions, while the remaining contain surfactants and co-solvents. Type II contains lipophilic surfactants with low (<12) hydrophilic-lipophilic balance (HLB) values, whereas IIIA/IIIB and IV contains surfactants with higher HLB values (>11). Type IIIA and IIIB are distinguished from each other by digestible lipid content, with IIIA ranging between 40 and 80% and IIIB containing less than 20%. Type IV formulations are generally not considered digestible as they contain only surfactants and co-solvents. Solubility of API in the undispersed formulation from each class typically increases with the LFCS number, but type IV formulations typically incur the highest risk of precipitation once the LBF is dispersed in an aqueous medium.[24(p4)] The LFCS can be further extended by the type of digestible lipid that is used, for example medium-chain (MC) and long-chain (LC).

The selected LBFs (Table 1) are thus representative of self-emulsifying formulations, with very similar compositions but differing solvation and solubilization capacities for fenofibrate. LBFs were prepared as described previously.[15] Briefly, excipients were weighed into glass vials, sealed, vortexed, and placed on a shaker (300 rpm) at 37 °C for 24 h. Subsequently, they were loaded with 80 mg fenofibrate per gram LBF. This loading corresponded to 55.6, 82.8, and 76.6% of equilibrium solubility at 37 °C for LBF types IIIA-MC, IIIA-LC, and IV, respectively.[21]

Artificial Membrane Preparation

The LiDo artificial membrane was prepared as previously described.[5] Briefly, 2 g lecithin extract (Avanti's "Soy PC (20%)") was dissolved in *n*-dodecane with 1.5% (v/v) ethanol to a final volume of 10 mL. Insoluble material was removed by centrifugation (20 min, 3220 *g* at room temperature), and the supernatant (LiDo membrane-forming solution) aliquoted for single-use and capped with nitrogen prior to freezing (−18 °C). The day before an experiment, aliquots were thawed at room temperature. LiDo membranes were prepared 10 min prior to the experiments by coating polyvinylidene difluoride (PVDF) filter supports (Millipore Immobilon-P, 0.45 μm pore size, ~70% pore area) with 16.2 μL per cm^2 of filter (total area: 44 cm^2).

Table 1
Formulation composition and excipient properties.

LBF type[a]	Digestible lipid excipients	Proportion (% w/w)	C:D[b]	Surfactant excipients	Proportion (% w/w)
IIIA-MC	Miglyol 812 N	40	8:0, 10:0	Tween 85	40
				Kolliphor RH40	20
IIIA-LC	Olive oil	40	18:1–2, 16:0	Tween 85	40
				Kolliphor RH40	20
IV	–	–	–	Tween 85	67
				Kolliphor RH40	33

[a] Lipid-based formulation (LBF) type based on the Lipid Formulation Classification System and lipid chain length, as either medium chain (MC) or long chain (LC).
[b] Number of carbons (C) and non-saturated carbons (D) in the acyl chains of the digestible lipids comprising the formulation.

Cellular Monolayer Preparation

Caco-2 cells (American Type Culture Collection, VA, USA) were cultivated in an atmosphere of 90% air and 10% CO_2 as described previously.[18] Briefly, Caco-2 cells (passage 95–105) were seeded on permeable polycarbonate filter supports (0.45 μm pore size, 75 mm diameter; Transwell Costar, Sigma-Aldrich) at a density of 170 000 cells/cm^2 in Dulbecco's modified Eagle's medium (DMEM) supplemented with 10% fetal calf serum, 1% minimum essential medium non-essential amino acids, penicillin (100 U/mL), and streptomycin (100 μg/mL). Monolayers were used between day 21 and 26 after seeding.

MDCK II cells (American Type Culture Collection, VA, USA) were cultivated, at 37 °C in an atmosphere of 95% air and 5% CO_2, at 95% relative humidity, as described previously.[20] Briefly, the cells were seeded on permeable polycarbonate filter supports at densities of 113 000 and 170 000 cells/cm^2 in DMEM containing Glutamax and 10% fetal bovine serum to establish the required seeding density. Monolayers were used for experiments on day 4 after seeding. MDCK II will be referred to as MDCK cells throughout the rest of the manuscript.

In vitro *Lipolysis-permeation*

Lipolysis-permeation was performed as described previously, using Titrando (Metrohm, Switzerland) equipment with automated pH-titration and propeller stirring (450 rpm) of the donor medium and a magnetic bar stirring the receiver chamber.[15] The donor medium (60 mL) was prepared by dissolving FaSSIF/FeSSIF/FaSSGF powder (2.24 g/L) to obtain 3 mM taurocholate and 0.75 mM lecithin in lipolysis buffer (pH 6.5, 2 mM Tris-maleate, 150 mM NaCl, and 1.4 mM $CaCl_2$).

The donor compartment was separated from the receiver compartment by either the Caco-2 or MDCK monolayer seeded on polycarbonate filters, or in the cell-free conditions, a LiDo artificial membrane (on a PVDF filter). The receiver compartment contained 235 mL HBSS buffered with 25 mM HEPES (pH 7.4), and supplemented with 4% (w/v) BSA. Membrane integrity was evaluated by monitoring either the Lucifer yellow (LY) permeation across the monolayers or the pH in the donor compartment, as described previously.[15]

Distribution During Dispersion and Digestion of Fenofibrate-loaded LBFs

Fenofibrate-loaded LBF (1.5 g) was dispersed in the donor medium (60 mL) and the pH manually adjusted to 6.5 with 0.1 M NaOH. After 10 min of dispersion, 750 mg of Novozym 435 was added to initiate the digestion. A 0.2 M NaOH solution maintained the donor pH at 6.5 by autotitration during the digestions of the IIIA-LC and IV LBFs; 0.6 M NaOH was used during digestion of the IIIA-MC formulation.

Samples were taken from both compartments at 0, 5, 10, 15, 20, 30, 40, 50, 60 min after addition of lipase. In the donor samples, digestion was inhibited by addition of 5 μL/mL of a 4-bromophenol boronic acid solution (0.5 M in methanol). These samples were immediately centrifuged at 21 000 *g* (10 min, 37 °C) to pellet undissolved fenofibrate. The supernatant was analyzed with dynamic light scattering. These samples were then diluted 100-fold in mobile phase, and centrifuged at 21 000 *g* (10 min, 20 °C) for HPLC-UV analysis. The precipitated fenofibrate was resuspended in an equal volume of acetonitrile by vortexing, then centrifuged at 21 000 *g* (10 min, 20 °C) to remove remaining insoluble material. Thereafter, this supernatant was diluted 10-fold in mobile phase for HPLC-UV analysis. Samples obtained from the receiver compartment were diluted 4-fold with cold acetonitrile and vortexed to precipitate BSA. After centrifugation at 21 000 *g* (10 min, 4 °C), the supernatants were diluted 5-fold in a solution of 43.8% (v/v) acetonitrile in water and 1.25 nM warfarin (internal standard) for UPLC-MS/MS analysis.

Sample Analysis

Fluorescence

LY was detected using fluorescence in a Spark plate reader (Tecan, Austria) at 428 nm (excitation) and 536 nm (emission). Samples were diluted 4-fold in ice-cold acetonitrile and centrifuged at 21 000 *g* (4 °C) for 20 min to precipitate protein content.

HPLC-UV

All donor samples were analyzed for fenofibrate using a UV-DAD coupled HPLC (1290 Infinity, Agilent Technologies) with a Zorbax Eclipse XDB-C18 column (4.6 × 100 mm, Agilent Technologies), kept at 40 °C. Injection volume was 20 μL. The mobile phase consisted of 20% (v/v) 25 mM sodium acetate buffer, pH 5.0 in acetonitrile and an isocratic flow at 1 mL/min was used. UV absorbance was monitored at 287 nm. The retention time of fenofibrate was 3.32 min.

UPLC-MS/MS

UPLC-MS/MS analysis was performed using a Xevo TQ-S MS coupled Acquity UPLC system (Waters, Milford, MA) with a BEH C18 column (2.1 × 50 mm, 1.7 μm, Waters). The mobile phase consisted of 5% acetonitrile and 0.1% formic acid in water (solvent A), and 0.1% formic acid in acetonitrile (solvent B). Gradient elution at a constant flow rate of 0.5 mL/min was used. Mobile phase A was constant (95%) from 0 to 0.5 min, followed by linear decrease to 10% until 1.2 min, constant flow for 0.4 min, and then linear increase back to 95% A at 1.6 min until the end of the run (2 min, injection volume 7.5 μL). The column oven and auto-sampler tray temperature were set at 60 °C and 10 °C, respectively.

The mass spectrometer was operated in positive electrospray mode for fenofibrate and fenofibric acid to analyze receiver samples, and in negative mode for taurocholate. Warfarin was used as internal standard. The retention times were 1.63 (fenofibrate), 1.43 (fenofibric acid), 1.29 (taurocholate) and 1.37 min (warfarin). Precursor-product ion pairs were: (i) *m/z* 361 → 233 (cone voltage 20 and collision energy 16 V) for fenofibrate; (ii) *m/z* 319 → 139 (cone voltage 20 and collision energy 32 V) for fenofibric acid; (iii) *m/z* 514 → 123 (cone voltage 50 and collision energy 50 V) for taurocholate; (iv) *m/z* 309 → 163 (cone voltage 22 and collision energy 14 V) for warfarin in positive mode; and (v) *m/z* 307 → 161 (cone voltage 40 and collision energy 22 V) for warfarin in negative mode. Data acquisition and peak integration were performed with MassLynx software (Waters).

Droplet Size Determination

Samples from the donor chamber of the lipolysis-permeation experiments were analyzed with dynamic light scattering (DLS) to obtain the droplet size distribution. Samples were centrifuged to remove precipitated fenofibrate (as described above). The time from sampling to DLS analysis was within 20 min, during which the samples were kept at 37 °C. The supernatant (aqueous phase), 60 μL, was added to a low-volume quartz cuvette (Hellma Analytics, Germany) and analyzed with a Litesizer 500 (Anton Paar, Austria) DLS, equipped with a laser at a wavelength of 658 nm. The determinations were performed at 37 °C after 1 min equilibration, at a measurement angle of 175° The solvent refractive index was set to 1.3304 and viscosity to 0.7073 mPa·s, corresponding to a 154 mM NaCl solution in the Kalliope software version 2.8.3 used to operate the instrument and process the data (Anton Paar, Austria).

Data Analysis

Data are presented as mean values with standard deviation ($n \geq 3$, unless otherwise specified). Our Caco-2 fenofibrate data came from a previous study (n = 3).[15] The experiments from our current study were solely used to study the flux of taurocholate and colloidal structure size in the digestion chamber. Supersaturation was calculated using drug solubility in the aqueous phase of dispersed and digested blank formulations, as determined previously.[15] Permeation of fenofibrate was calculated by including the amount of fenofibric acid appearing in the receiver chamber, as enzymes present in the cells hydrolyze the fenofibrate to variable extents.

Statistical analysis was performed in GraphPad Prism 9.0.0 (GraphPad Software, USA). Differences between groups were evaluated by one-way ANOVA followed by a Tukey's multiple comparison analysis test. Two-way ANOVA followed by a Tukey's multiple comparison analysis test was used to compare groups with two differing factors (formulation and barrier model). P-values < 0.05 were considered statistically significant. Area under the curve (AUC) was calculated *via* a Python (version 3.8.3) script by fitting data to Akima splines using scipy.interpolate.Akima1DInterpolator and integrated using scipy.integrate.IntegrateQuad (SciPy version 1.5.1).

Formulation rankings between different assay models were compared by normalizing AUC values of concentration-time curves reflecting the: (i) donor chamber, (ii) receiver chamber, or (iii) *in vivo* plasma. Normalization was done by converting AUC values into percentages of the group sum, where 100% was defined as the sum of mean values in each respective group.

Results

Membrane Integrity MDCK Monolayers

During the initial exploration of the MDCK cell line for use in lipolysis-permeation assays, two seeding densities were studied in the lipolysis-permeation setup: 113 000 and 170 000 cells/cm^2. These monolayers were subjected to increasingly complex donor media and the pH in the donor compartment and LY permeation were monitored to evaluate monolayer integrity. The lower density was compatible with the donor media but only withstood the type IV formulation for 40 min. The monolayers cultured with the high seeding density were more resilient. For the type IV formulation, the LY flux was low and no pH increase was observed for 100 min. However, for the IIIA formulations, loss of barrier function occurred after 40 min. Therefore, further experiments with MDCK cells were performed with cells seeded at a density of 170 000 cells/cm^2 and the lipolysis-permeation experiments lasted a total of 40 min.

Fenofibrate Distribution in the Lipolysis-permeation Setup

MDCK Monolayer

Fenofibrate distribution across phases in the donor compartment with MDCK monolayers showed clear distinction between the types of LBF (Fig. 1). The type IV LBF maintained aqueous fenofibrate concentrations relatively well, until approximately 10 min after the lipolysis was initiated. At this point, the solubilized concentration dropped significantly ($p < 0.05$). Conversely, no decrease in solubilization during lipolysis was observed for the other formulations. Supersaturation ratios dropped during the first 10–20 min before stabilizing for the type IV and IIIA-LC LBFs, whereas the supersaturation ratio appeared to increase again at the 25 min mark for the IIIA-MC formulation. In the MDCK absorption model, the mass transfer rate of fenofibrate across the cell monolayer was significantly higher ($p < 0.02$) when loaded in the type IV LBF, compared to the other formulations (Fig. 1d). The proportion of fenofibric acid to fenofibrate in the receiver media was negligible, generally below 3%.

LiDo Artificial Membrane

The distribution of fenofibrate across the aqueous and solid phase in the donor media (Fig. 2) using the LiDo was very similar to the cell-based alternative, except that solubilization level of fenofibrate occurred 5 min sooner when loaded in the type IV LBF. Another exception was the profile of precipitated fenofibrate (Fig. 2b) decreasing at 15 min and onwards, though this was not mirrored by the solubilization profile. No significant differences between mass transfer rates of fenofibrate across the artificial membrane were observed in the different formulation conditions. In the absence of cells, no fenofibric acid was found in the receiver media and all compound was recovered as fenofibrate.

IVIVR Fenofibrate: Pigs and Absorption Membranes

In order to establish an *in vitro – in vivo* relationship (IVIVR), the time profiles for fenofibrate mass transfer across the absorption barriers were integrated to calculate their AUC. Plasma concentrations from pigs, obtained from a previous study by Griffin et al.,[21] were treated in the same way. After normalizing the AUCs within their model groups, the AUC values were compared with each other (Fig. 3). There was no significant difference between the formulations in either the Caco-2 and LiDo absorption models, when looking at absorption of fenofibrate and fenofibric acid as a composite. However, the MDCK model significantly overestimated the performance of the type IV LBF compared to *in vivo* plasma exposure. No differences between the medium-chain or long-chain type IIIA LBFs were seen in any of the *in vitro* models.

Permeation of Taurocholate and Colloidal Structure Size

Permeation of taurocholate and colloidal structure size changes were also studied during lipolysis-permeation experiments with the different absorption membranes. The flux of taurocholate in the Caco-2 and MDCK experiments was significantly higher than in the LiDo experiments. However, the absolute amount permeated was still negligible and did not exceed 0.04% of the donor media amount. It is therefore unlikely that taurocholate absorption has any effect on the *in vitro* results (Fig. S1).

The size distribution of the colloidal emulsion droplets in the donor compartment was measured at each sampling point (Fig. S2, table S1) to determine whether it correlated to permeation of either fenofibrate or taurocholate during lipolysis, and whether the choice of absorptive membrane affected these auxiliary *in vitro* assay parameters. No significant differences were observed for the different absorption membranes. However, the dispersion and digestion of type IV LBFs resulted in much larger droplet sizes, which varied over the course of the experiments. When dispersing the formulation inside a vial via vortex mixing, the droplets had a hydrodynamic diameter of 146 nm. However, after 10 min of dispersion via overhead stirring in the ENA device, the droplet size was 363–422 nm. It then diminished over 10–20 min to 235–318 nm. Furthermore, the distribution was bimodal, with the co-existence of a smaller volume of larger structures (>250 nm) and greater one of smaller structures (<50 nm). No such time-dependent trends were seen for the type IIIA formulations, where the droplet size was consistently 55–98 nm with a monomodal distribution.

Discussion

In order to address the poor *in vitro* predictability of *in vivo* LBF performances,[4,7,8] we have recently developed the first *in vitro*

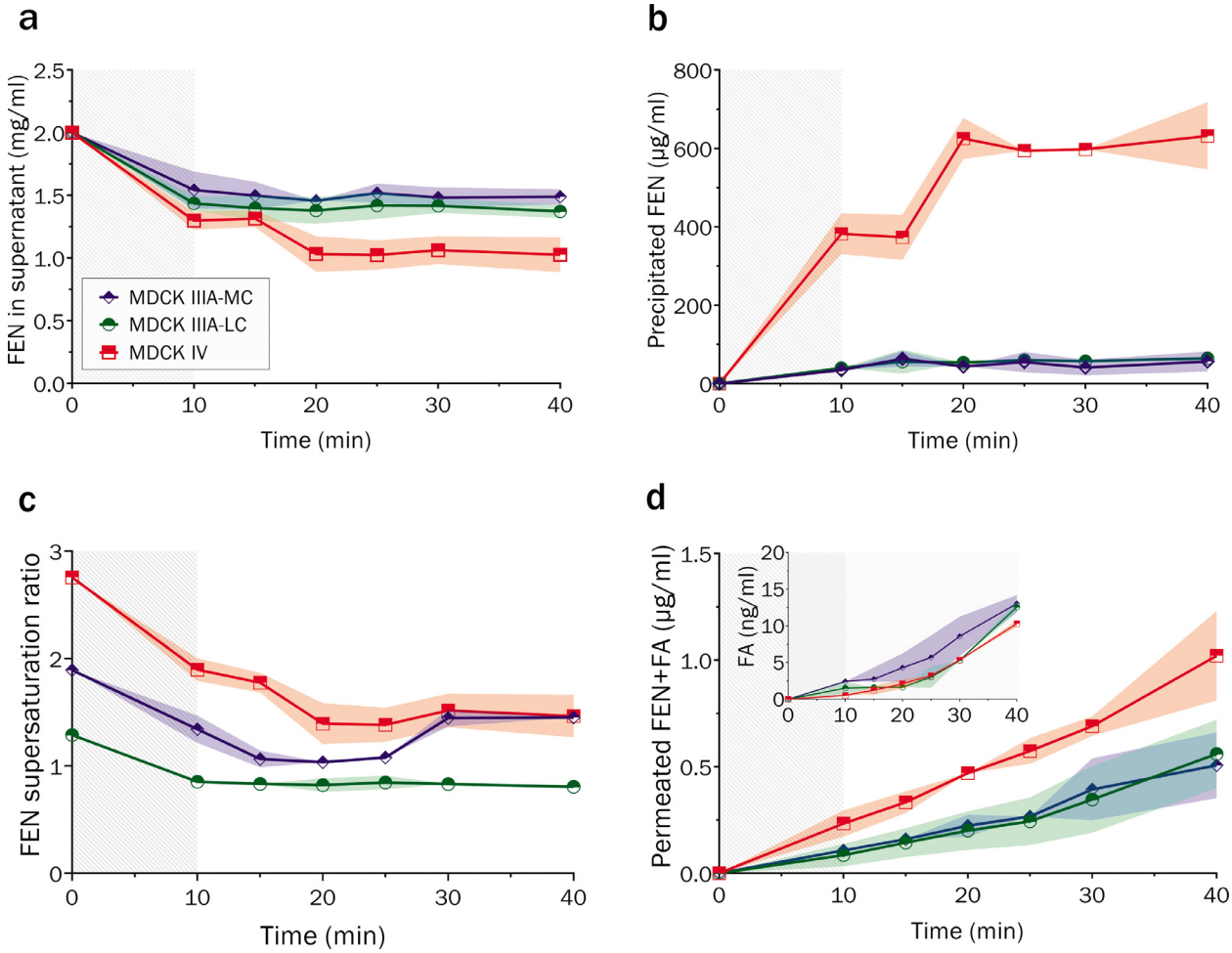

Fig. 1. Fenofibrate disposition over time during lipolysis-permeation experiments of drug-loaded type IIIA-MC (□ diamonds), IIIA-LC (◓ circles) or IV (□ squares) LBFs, performed with MDCK monolayers as absorption membrane. The gray and white areas indicate dispersion and digestion phases, respectively. Shaded trace outlines show the standard deviation. (**a**) Fenofibrate concentration in the aqueous phase the of donor compartment. (**b**) Concentration of fenofibrate solids (precipitate) in the donor compartment. (**c**) Supersaturation ratios in the donor media (**d**) Fenofibrate concentrations (μg/mL) measured in the receiver chamber as a composite of FEN and fenofibric acid (FA). Insert shows concentrations (ng/mL) of FA only.

lipolysis-permeation setup which captures the complex interplay between intestinal digestion and absorption.[15,16] Drug permeation across a Caco-2 membrane accurately reproduces *in vivo* absorption profiles of several LBFs in landrace pigs and Labrador dogs.[15,17] The current study demonstrates that lipolysis-permeation experiments using artificial LiDo membranes also accurately reflected the *in vivo* performance for the three fenofibrate-loaded LBFs in landrace pigs, whereas the MDCK membranes did not (Fig. 3).

In previously published Caco-2 model data, there was a clear distinction in fenofibrate distributions across the different phases in the donor media, when the three LBFs were dispersed and digested in the lipolysis-permeation setup.[15] Especially the type IV LBF was distinguished by a lower solubilizing capacity for fenofibrate, leading to more precipitation than with the other two LBFs. Digestion did not appear to have a strong effect as no obvious changes occurred after initiation of lipolysis. The fenofibrate mass transfer across the Caco-2 monolayer was not significantly different between the formulations.

The LiDo membrane is compatible with the harsh lipolysis conditions, even when porcine pancreatin is used for the digestion.[5] The current study used immobilized lipase since cell-based models do not withstand pancreatic extract,[25] and we aimed to directly compare the different absorption membranes. In addition, porcine pancreatin at high lipase activity did not result in accurate predictions of LBF performance, based on lipolysis-permeation assays with the LiDo artificial membrane.[5] Overall, the drug distribution in the digestion medium during the previous Caco-2 and current LiDo experiments was similar (Fig. 4). One notable exception was the precipitation observed for the IV formulation, which could be caused by fenofibrate partitioning into the LiDo membrane. A slightly higher permeation was also observed across the LiDo membrane for the type IIIA-LC formulation. Interactions between the excipients, the immobilized lipase, digestion products, and the absorption membranes may have caused this minor difference. In addition, solubilization, supersaturation and precipitation levels might change during sampling and phase separation (*i.e.,* sampling handling and centrifugation) and are therefore not likely to accurately reflect the concentration of free drug in the donor compartment available for absorption.[15,26] The composition and solubilizing capacity of the colloidal structures formed in the donor chamber during digestion constantly change as they depend on the composition of the LBFs and the digestion products formed.[15,27] This drives differences in free drug availability which is reflected by how much of the compound permeates the absorption membrane.

Permeation is therefore the main parameter of interest. Since fenofibrate is a lipophilic compound, absorbed mainly by passive diffusion, it was expected that the LiDo membrane experiments

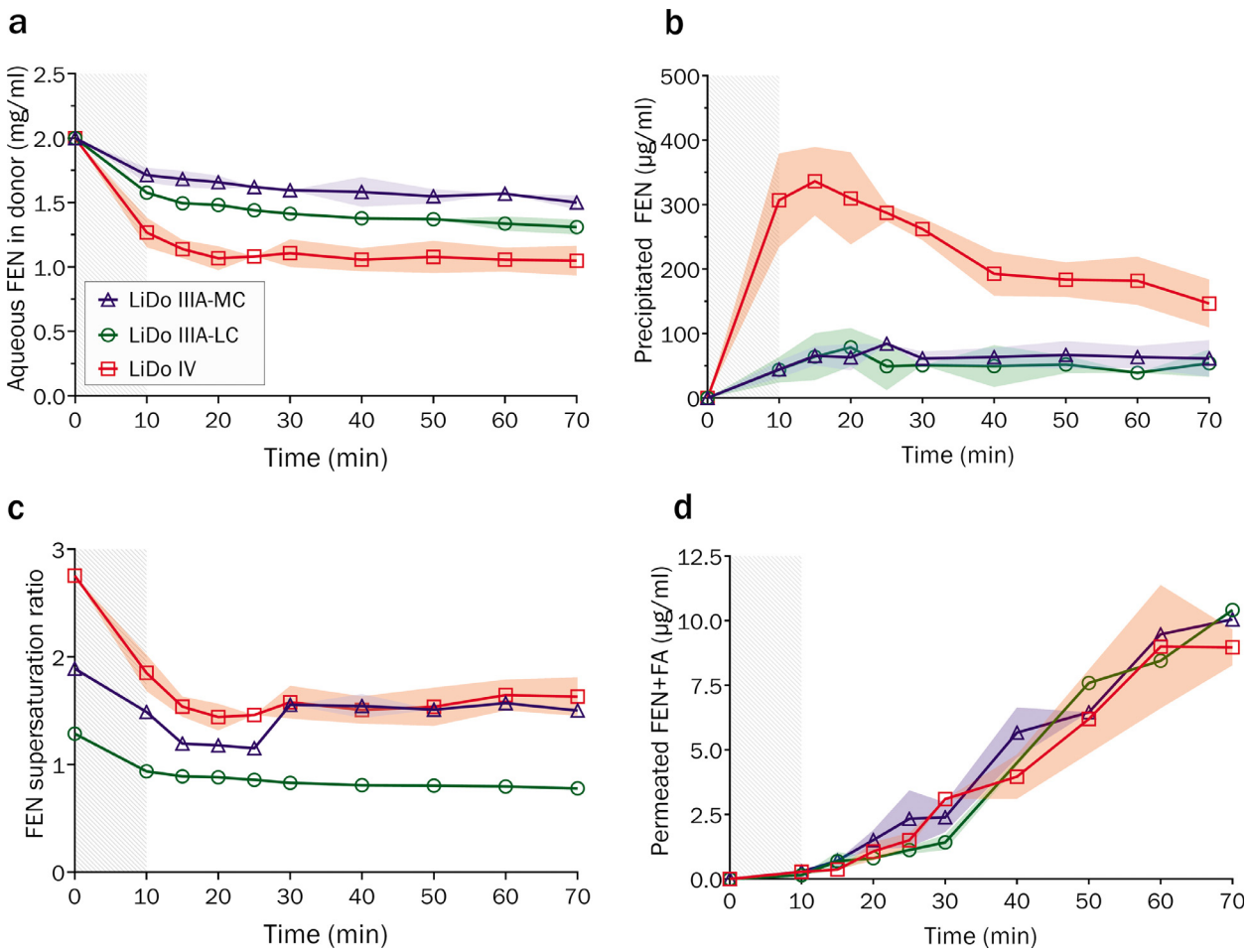

Fig. 2. Fenofibrate (FEN) disposition over time during lipolysis-permeation experiments of drug-loaded type IIIA-MC (◇ triangles), IIIA-LC (○ circles) or IV (□ squares) LBFs, performed with LiDo as absorption membrane. The gray and white areas indicate dispersion and digestion phases, respectively. Shaded trace outlines show the standard deviation. (**a**) Fenofibrate concentration measured in the aqueous phase of the donor compartment. (**b**) Concentration of fenofibrate solids (precipitate) in the donor compartment. (**c**) Supersaturation ratios in the donor media.[15] (**d**) Fenofibrate concentrations measured in the receiver chamber.

accurately predicted that all formulations performed similarly *in vivo*.[21] There are major advantages of the artificial membrane in that it: (i) is readily available, (ii) does not require cell culture facilities, and (iii) is cheaper than cell-based assays. Moreover, it has the potential to be used in different (dissolution-) permeation setups and potentially predict drug absorption for other kinds of enabling formulations.[2] The analogous GIT-0 membrane has for example been used in the μFlux apparatus to correctly predict the rank order of the exposure of non-digestible enabling formulations containing itraconazole as well as food effects using fasted and fed state simulated intestinal fluids.[28,29] A drawback of the LiDo membrane in the lipolysis-permeation setup is that the membranes seem to affect the pH probe over time. A potential solution could be to use a stronger buffer in the digestion chamber instead of the pH-stat, a strategy we have successfully used in a different experimental setup.[30] A stronger buffer would also allow for reduction of the donor volume in the current setup by up to 67% and therefore increasing the surface-area to donor volume ratio (A/V) by the same amount.

The current study also evaluated the use of MDCK cells as an absorption membrane in the lipolysis-permeation setup. This cell line has gained popularity for permeability assays within academia and industry.[31] MDCK cells are derived from kidney epithelia and form monolayers similar to the epithelial cells found in the small intestine. Although this cell line is of canine origin, the cells can be humanized by knocking out canine transporters such as cMDR1 and

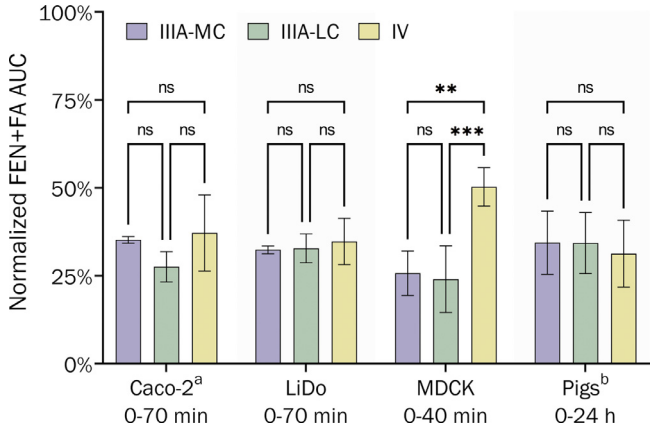

Fig. 3. Comparison of LBF performance between the three absorption models (Caco-2, LiDo, and MDCK) for *in vitro* lipolysis-permeation, and an *in vivo* pig model.[21] Exposure of fenofibrate over time shown as AUC (area under curve), comprising the compounded receiver exposure of fenofibrate (FEN) and fenofibric acid (FA) for Caco-2 and MDCK (partial intracellular hydrolysis). The LiDo only included FEN (no intracellular hydrolysis) and in pig plasma only FA was included (complete hydrolysis after absorption). Values are normalized as percentage of group sum for comparison, where each absorption model constitutes a group. [a]Data from Keemink et al. (2019), included for comparison.[15] [b]Data from Griffin et al. (2014).[21] Error bars show the standard deviation, and asterisks denote level of significance ($^{*}p < 0.05$, $^{**}p < 0.01$, $^{***}p < 0.001$).

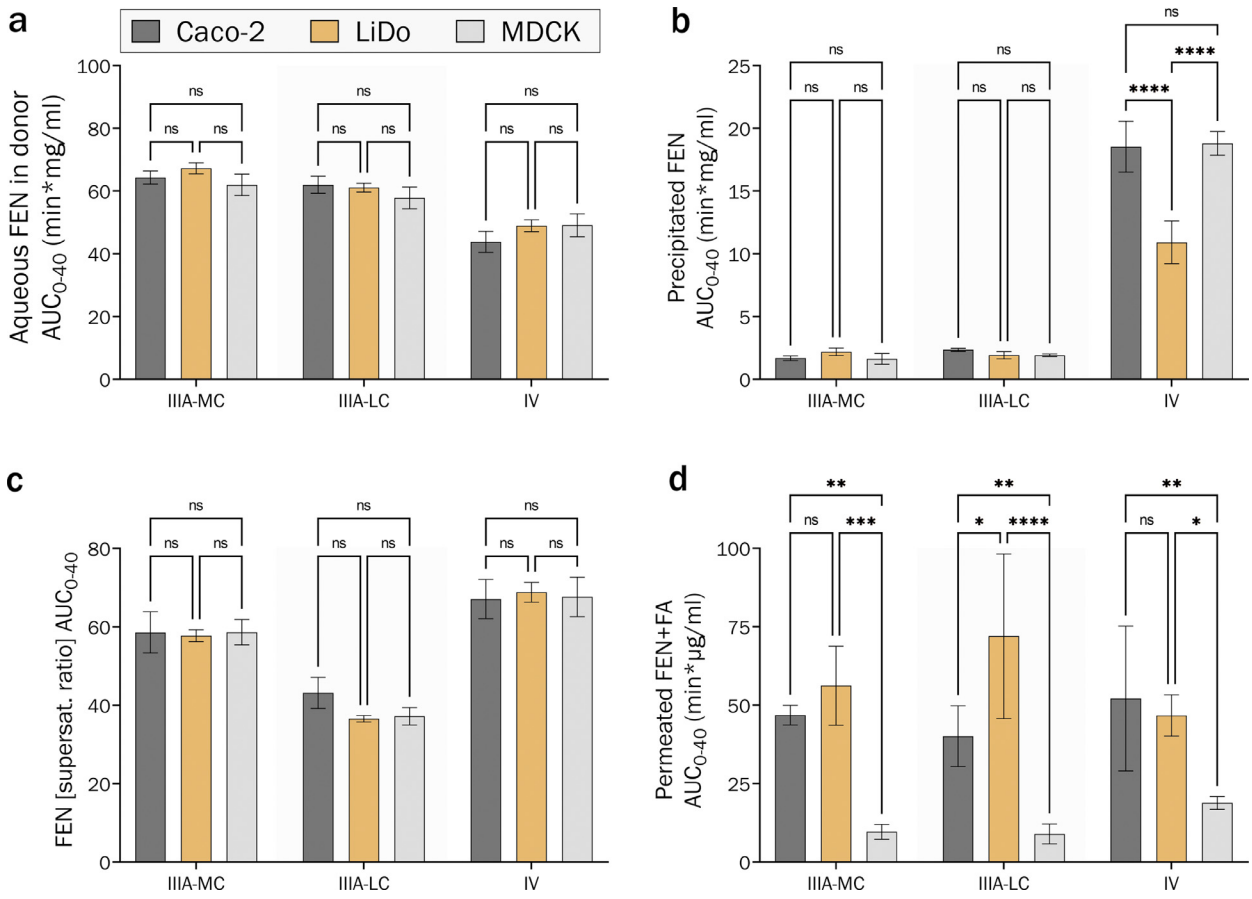

Fig. 4. Comparison between *in vitro* absorption membrane models: Caco-2 (■), MDCK (□), and LiDo (■). Exposure over time shown as $AUC_{0-40\ min}$ (area under curve) for different fenofibrate (FEN) fractions and LBF types (IIIA-MC, IIIA-LC, and IV). AUCs calculated from: (**a**) FEN concentration in the aqueous phase of the donor compartment. (**b**) Concentration of FEN solids (precipitate) in the donor compartment. (**d**) Supersaturation ratios determined in the donor compartment. (**d**) Composite FEN and fenofibric acid (FA) concentrations measured in the receiver chamber. Caco-2 data from Keemink et al. (2019), included for comparison.[15] Error bars show the standard deviation, and asterisks denote level of significance ($^{*}p < 0.05$, $^{**}p < 0.01$, $^{***}p < 0.001$, $^{****}p < 0.0001$).

knocking in human transporters, *e.g.,* hMDR1.[20,32] A major drawback of the Caco-2 model is that it does not express transporters to the extent found in the small intestine, *i.e.,* ASBT, MRP3, OCT1 and OCT3.[33] Therefore, MDCK cells could be a better alternative for drug compounds that are transporter substrates. The apparent permeability coefficients (P_{app}) in MDCK cells correlate well with those in Caco-2 cells and the Spearman's rank correlation coefficient for MDCK P_{app} and human absorption is comparable to the value for Caco-2 cells.[34] However, permeation of fenofibrate across the kidney cell line did not reflect *in vivo* exposure in the present study. Our experiments with the type IV LBFs showed significantly higher fenofibrate permeation than the other two formulations (Fig. 4). In general, MDCK cells were less resistant to the lipolysis conditions than the Caco-2 cells and we therefore only performed experiments for 40 min. Although membrane integrity was closely monitored using LY and the pH gradient, we cannot exclude the possibility that MDCK absorption barriers were affected by the relatively high concentration of surfactants in the type IV formulation. In general, little is known about the interaction between LBF surfactants and MDCK monolayers. Hanke et al. found that low concentrations of Kolliphor RH40 (up to 0.5%) does not affect cell viability or permeability of the paracellular marker calcein.[35] Similarly, Bunchongpraset and Shao reported that Kolliphor RH40 in concentrations up to 2% (w/v) does not affect cell permeability in 1:1 formulations with lipids.[36] However, to the best of our knowledge, the effect of the major component of the type IV LBF, Tween 85, has not been studied on MDCK cell membranes. It has been reported that detrimental effects of mixed glycerides diminishes in the presence of triglycerides, which are present in both the IIIA formulations.[36] Interestingly, the permeation across the MDCK cells was lower than in the Caco-2 cells (Fig. 4). One of the differences was that only the prodrug fenofibrate—and almost no fenofibric acid—was detected in the receiver chamber during the MDCK experiments. In our previously reported Caco-2 experiments, fenofibric acid concentration at the 40 min mark was 3.3 ± 1.9 times higher than the fenofibrate concentration. These differences can be explained by limited esterase expression in the kidney cell line. Fenofibrate is a substrate of the hepatic carboxylesterase CES1, which, has been reported to be expressed in MDCK II cells in other labs,[37] but not in the MDCK cells used in our lab.[32] Conversely, expression of CES1 in the colonic cell line is a well-known phenomenon,[38] and confirmed as highly expressed in the Caco-2 cells used in the previous study.[39] In healthy human small-intestinal mucosa however, the CES2 isoform is the most prevalent.[40] Fenofibrate would appear to be a better substrate for CES1 than for CES2, and is in fact a potent inhibitor of CES2.[41] Nonetheless, the artificial membrane lacks enzyme activity and still performed comparably to the Caco-2 cells.

The artificial membrane is entirely lipophilic. It stands to reason that flux into the receiver medium should therefore be quite high, once the membrane is saturated with fenofibrate. For permeation through cell monolayers however, the compound must transit from a lipid phase (apical membrane) to an aqueous one (cytosol), then to a second lipid phase (basolateral membrane) before entering the

receiver medium. If fenofibrate is hydrolyzed into fenofibric acid in the cytosol, the equilibrium solubility of the acid will be significantly higher than the ester. For a cell monolayer with low esterase activity (MDCK), the low aqueous solubility of fenofibrate might severely limit the rate of permeation, with the transition from apical membrane to cytosol being the rate-limiting step. In the Caco-2 cells, CES1 will continuously remove fenofibrate from the cytosol by hydrolysis into the more soluble acid, and therefore create a stronger concentration gradient between the apical membrane and cytosol. This, in turn, provides a stronger membrane sink effect for Caco-2 than for MDCK for a lipophilic pro-drug such as fenofibrate. While the permeability of the acid through the basolateral membrane should be lowered due to ionization (pKa 3–4), the high concentration gradient between cytosol and basolateral membrane might compensate for this. Pretreatment of Caco-2 monolayers with a CES1 inhibitor such as benzil, mevastatin or tamoxifen,[42] could be a relatively simple way of verifying the hypothesis regarding intracellular hydrolysis on fenofibrate flux. However, for further exploration of cellular monolayers in lipolysis-permeation assays, using model lipohilic drugs that are less susceptible to intracellular metabolism is recommended.

Based on the current and previous studies, the Caco-2 cells seem more suitable than the MDCK monolayers for (dissolution-)permeation systems that evaluate the performance of enabling formulations and LBFs in particular.[17,30,43,44] A strategy to protect the MDCK cells from potentially detrimental effects of the digestion medium could be a mucus layer on top of the membrane, as has been done with Caco-2 cells.[25] Falavigna et al. applied biosimilar mucus to an artificial PVPA barrier with the aim of simulating the intestinal mucosa. They also used fenofibrate as a model compound. In agreement with our findings, they found that the permeated compound reflected *in vivo* exposure whereas solubilized drug in the digestion medium did not.[11]

In addition to fenofibrate, we evaluated the permeation of taurocholate across the absorption membranes and LBF droplet size over the course of lipolysis. The structure of colloidal aggregates is affected by the concentration of the excipients and their digestion products. As digestion increases over time, the composition of solubilizing compounds in the medium changes from predominantly triglycerides (for the IIIA LBFs in this case) to predominantly monoglycerides and fatty acids. These are more soluble in water, more surface active, and more sensitive to pH. In the intestine, absorption of monoglycerides and free fatty acids occurs simultaneously with lipolysis, while tri- and diglycerides are generally not absorbed.[45] An important auxiliary solubilizing component in the intestinal fluid is bile, secreted from the gall bladder as response to cholecystokinin when lipids are present in the duodenum.[46] In this study, bile was represented by taurocholate present as a bolus from the start of the experiment and not continually secreted. Absorption of taurocholate from the donor medium *in vitro* could therefore hypothetically reduce the solubilizing capacity, and affect the colloidal structuring of the donor medium apart from lipolysis effects,[47] potentially more so than *in vivo*. However, as seen in the Results, a negligible amount of the bile salt permeated into the receive compartment (Fig. S1). There is therefore little evidence that the absorption membrane would affect the colloidal structures and the free fenofibrate concentrations, because of the disappearance of bile salt from the digestion medium. Absorption of fatty acids and monoglycerides could however have an effect on the colloidal structuring. As this is generally considered to be a facilitated process intestinally,[48] it is more likely to be seen for cell-based models *in vitro*. However, the insignificant change in size of the colloidal structures over time in this study and little difference between cell-based and cell-free models (Fig. S2), suggest limited effects of absorption and lipolysis on the colloidal structures. The DLS method used in this study is however a fairly crude measurement, which does not give any information on the structure apart from diffusivity in the medium, correlated to hydrodynamic radius of an assumed spherical structure. More informative methods such as synchrotron small angle x-ray scattering (sSAXS) or small angle neutron scattering (SANS) could therefore shed more light on this process. This has been done for *in vitro* lipolysis on many occasions, but generally not with simultaneous absorption.[22]

For the LiDo artificial membrane, we would expect limited absorption of lipid digestion products. For the cell monolayers however, provided that the lipid transport mechanisms are intact *in vitro*, the long-chain and medium-chain formulations may induce different effects. *In vivo*, short- and medium-chain lipids are absorbed via the portal vein to a much greater extent than long-chain lipids, which are predominantly absorbed via chylomicron incorporation and taken up in the lymph.[49] *In vitro* the long-chain formulations may induce a buildup of lipids in the cytosol as chylomicron secretion is less efficient in cell lines than in the intestine.[50,51] These processes could affect the observed results, such as reducing the flux of fenofibrate from the IIIA LBFs compared to the type IV LBF by sequestration of drug in intracellular lipid aggregates. Higher digestion rate of the medium-chain lipids might lead to higher absorption of digestion products and offset higher intracellular retention from long-chain lipids. Under the experimental conditions of this study, this could also serve to explain the inaccurate ranking of the LBFs. A higher degree of intracellular retention due to lipid buildup might be more noticeable when using MDCK monolayers than with Caco-2 monolayers due to fenofibrate partitioning into lipid aggregates to a higher extent than fenofibric acid would. Further studies into the use of MDCK monolayers for lipolysis-permeation assays is therefore warranted.

Although the cone shape of the lipolysis-permeation device was designed to optimize the A/V, less than 3% of the total fenofibrate crossed the LiDo membrane, or Caco-2 monolayers previously.[15] In order to better reflect the *in vivo* situation, this A/V ratio could be optimized, we briefly touched upon the strategy of further reducing the donor volume previously.[2] Similarly to what was done for the Caco-2 membrane, it would also be interesting to evaluate the proposed lipolysis-permeation setup using the LiDo membrane with other drug-delivery system types, *e.g.,* amorphous solid dispersions or mesoporous materials combined with lipids.[17] Additional studies on different LBFs are also required before any of the discussed absorption models can be reliably used for prediction of *in vivo* outcomes. As the reference study shows that the formulations are equivalent *in vivo*, comparison by linear regression is not feasible, however rank-order comparisons can still be made where agreement should consist of equal receiver AUC for each LBF *in vitro*. Nonetheless, a wide range of formulations and lipophilic drugs must be evaluated to give confidence to predictions from lipolysis-permeation assays.

Conclusion

We demonstrated that the artificial LiDo membrane is a promising tool in the lipolysis-permeation setup to evaluate the performance of LBFs. Like the Caco-2 membrane, it accurately gave the same drug permeation results for the three fenofibrate-loaded LBFs as the plasma exposure in Landrace pigs. Permeation of taurocholate and its effects on the size of colloidal structures was negligible for the Caco-2 cells and the LiDo membrane. Major advantages of the artificial membranes are that they are readily available and do not require cell culture equipment. MDCK monolayers, on the other hand, were too sensitive to the harsh conditions of the digestion medium in the current setting and monolayer integrity was only maintained for 40 min. In addition, for the formulations studied, fenofibrate permeation with the MDCK cells did not capture the *in vivo* ranking of the LBFs.

Acknowledgements

This work was supported by European Research Council Grant 638965. We gratefully acknowledge Filip Karlén for his support during the MDCK experiments.

Supplementary Materials

Supplementary material associated with this article can be found in the online version at doi:10.1016/j.xphs.2021.09.009.

References

1. Carrière F. Impact of gastrointestinal lipolysis on oral lipid-based formulations and bioavailability of lipophilic drugs. Biochimie. 2016;125:297–305. https://doi.org/10.1016/j.biochi.2015.11.016.
2. Vinarov Z, Abrahamsson B, Artursson P, et al. Current challenges and future perspectives in oral absorption research: an opinion of the UNGAP network. *Adv Drug Deliv Rev*. 2021;171:289–331. https://doi.org/10.1016/j.addr.2021.02.001.
3. Chatterjee B, Hamed Almurisi S, Ahmed Mahdi Dukhan A, Mandal UK, Sengupta P. Controversies with self-emulsifying drug delivery system from pharmacokinetic point of view. *Drug Deliv*. 2016;23(9):3639–3652. https://doi.org/10.1080/10717544.2016.1214990.
4. Feeney OM, Crum MF, McEvoy CL, et al. 50years of oral lipid-based formulations: provenance, progress and future perspectives. *Adv Drug Deliv Rev*. 2016;101:167–194. https://doi.org/10.1016/j.addr.2016.04.007.
5. Hedge OJ, Bergström CAS. Suitability of artificial membranes in lipolysis-permeation assays of oral lipid-based formulations. *Pharm Res*. 2020;37(6). https://doi.org/10.1007/s11095-020-02833-9.
6. Williams HD, Anby MU, Sassene P, et al. Toward the establishment of standardized *in vitro* tests for lipid-based formulations. 2. The effect of bile salt concentration and drug loading on the performance of type I, II, IIIA, IIIB, and IV formulations during *in vitro* digestion. *Mol Pharm*. 2012;9(11):3286–3300. https://doi.org/10.1021/mp300331z.
7. Kollipara S, Gandhi RK. Pharmacokinetic aspects and in vitro–in vivo correlation potential for lipid-based formulations. *Acta Pharm Sin B*. 2014;4(5):333–349. https://doi.org/10.1016/j.apsb.2014.09.001.
8. Thomas N, Richter K, Pedersen TB, Holm R, Müllertz A, Rades T. In vitro lipolysis data does not adequately predict the in vivo performance of lipid-based drug delivery systems containing fenofibrate. *AAPS J*. 2014;16(3):539–549. https://doi.org/10.1208/s12248-014-9589-4.
9. Crum MF, Trevaskis NL, Williams HD, Pouton CW, Porter CJH. A new *in vitro* lipid digestion - *in vivo* absorption model to evaluate the mechanisms of drug absorption from lipid-based formulations. *Pharm Res*. 2016;33(4):970–982. https://doi.org/10.1007/s11095-015-1843-7.
10. Dahan A, Hoffman A. The effect of different lipid based formulations on the oral absorption of lipophilic drugs: the ability of *in vitro* lipolysis and consecutive ex vivo intestinal permeability data to predict *in vivo* bioavailability in rats. *Eur J Pharm Biopharm*. 2007;67(1):96–105. https://doi.org/10.1016/j.ejpb.2007.01.017.
11. Falavigna M, Klitgaard M, Berthelsen R, Müllertz A, Flaten GE. Predicting oral absorption of fenofibrate in lipid-based drug delivery systems by combining in vitro lipolysis with the mucus-PVPA permeability model. *J Pharm Sci*. 2021;110(1):208–216. https://doi.org/10.1016/j.xphs.2020.08.026.
12. Klitgaard M, Müllertz A, Berthelsen R. Estimating the oral absorption from self-nanoemulsifying drug delivery systems using an in vitro lipolysis-permeation method. Pharmaceutics. 2021;13(4):489. https://doi.org/10.3390/pharmaceutics13040489.
13. Sadhukha T, Layek B, Prabha S. Incorporation of lipolysis in monolayer permeability studies of lipid-based oral drug delivery systems. *Drug Deliv Transl Res*. 2018;8(2):375–386. https://doi.org/10.1007/s13346-017-0383-6.
14. Stillhart C, Imanidis G, Griffin BT, Kuentz M. Biopharmaceutical modeling of drug supersaturation during lipid-based formulation digestion considering an absorption sink. *Pharm Res*. 2014;31(12):3426–3444. https://doi.org/10.1007/s11095-014-1432-1.
15. Keemink J, Mårtensson E, Bergström CAS. A lipolysis-permeation setup for simultaneous study of digestion and absorption *in vitro*. *Mol Pharm*. 2019;16(3):921–930. https://doi.org/10.1021/acs.molpharmaceut.8b00811.
16. Bergström CAS, Keemink J. *In vitro* intestinal drug disposition device. Patent EP 3678638 B1. 2021.
17. Alskär LC, Parrow A, Keemink J, Johansson P, Abrahamsson B, Bergström CAS. Effect of lipids on absorption of carvedilol in dogs: is coadministration of lipids as efficient as a lipid-based formulation? *J Control Release*. 2019;304:90–100. https://doi.org/10.1016/j.jconrel.2019.04.038.
18. Hubatsch I, Ragnarsson EGE, Artursson P. Determination of drug permeability and prediction of drug absorption in Caco-2 monolayers. *Nat Protoc*. 2007;2(9):2111–2119. https://doi.org/10.1038/nprot.2007.303.
19. Bohets H, Annaert P, Mannens G, et al. Strategies for absorption screening in drug discovery and development. *Curr Top Med Chem*. 2001;1(5):367–383. https://doi.org/10.2174/1568026013394886.
20. Simoff I, Karlgren M, Backlund M, et al. Complete knockout of endogenous Mdr1 (Abcb1) in MDCK cells by CRISPR-Cas9. *J Pharm Sci*. 2016;105(2):1017–1021. https://doi.org/10.1016/S0022-3549(15)00171-9.
21. Griffin BT, Kuentz M, Vertzoni M, et al. Comparison of *in vitro* tests at various levels of complexity for the prediction of *in vivo* performance of lipid-based formulations: case studies with fenofibrate. Eur J Pharm Biopharm. 2014;86(3):427–437. https://doi.org/10.1016/j.ejpb.2013.10.016.
22. Vithani K, Jannin V, Pouton CW, Boyd BJ. Colloidal aspects of dispersion and digestion of self-dispersing lipid-based formulations for poorly water-soluble drugs. *Adv Drug Deliv Rev*. 2019;142:16–34. https://doi.org/10.1016/j.addr.2019.01.008.
23. Pouton CW. Lipid formulations for oral administration of drugs: non-emulsifying, self-emulsifying and 'self-microemulsifying' drug delivery systems. *Eur J Pharm Sci*. 2000;11(2):S93–S98. https://doi.org/10.1016/S0928-0987(00)00167-6.
24. Williams HD, Sassene P, Kleberg K, et al. Toward the establishment of standardized in vitro tests for lipid-based formulations, Part 4: Proposing a new lipid formulation performance classification system. *J Pharm Sci*. 2014;103(8):2441–2455. https://doi.org/10.1002/jps.24067.
25. Keemink J, Bergström CAS. Caco-2 cell conditions enabling studies of drug absorption from digestible lipid-based formulations. *Pharm Res*. 2018;35(4). https://doi.org/10.1007/s11095-017-2327-8.
26. Miller JM, Beig A, Carr RA, Webster GK, Dahan A. The solubility-permeability interplay when using cosolvents for solubilization: revising the way we use solubility-enabling formulations. *Mol Pharm*. 2012;9(3):581–590. https://doi.org/10.1021/mp200460u.
27. Tanaka Y, Nguyen T-H, Suys EJA, Porter CJH. Digestion of lipid-based formulations not only mediates changes to absorption of poorly soluble drugs due to differences in solubilization but also reflects changes to thermodynamic activity and permeability. *Mol Pharm*. 2021;18(4):1768–1778. https://doi.org/10.1021/acs.molpharmaceut.1c00015.
28. Borbás E, Kádár S, Tsinman K, et al. Prediction of bioequivalence and food effect using flux- and solubility-based methods. *Mol Pharm*. 2019;16(10):4121–4130. https://doi.org/10.1021/acs.molpharmaceut.9b00406.
29. Tsinman K, Tsinman O, Lingamaneni R, et al. Ranking itraconazole formulations based on the flux through artificial lipophilic membrane. *Pharm Res*. 2018;35(8). https://doi.org/10.1007/s11095-018-2440-3.
30. Alvebratt C, Keemink J, Edueng K, Cheung O, Strømme M, Bergström CAS. An *in vitro* dissolution–digestion–permeation assay for the study of advanced drug delivery systems. *Eur J Pharm Biopharm*. 2020;149:21–29. https://doi.org/10.1016/j.ejpb.2020.01.010.
31. Volpe DA. Drug-permeability and transporter assays in Caco-2 and MDCK cell lines. *Future Med Chem*. 2011;3(16):2063–2077. https://doi.org/10.4155/fmc.11.149.
32. Karlgren M, Simoff I, Backlund M, et al. A CRISPR-Cas9 generated MDCK cell line expressing human MDR1 without endogenous canine MDR1 (cABCB1): an improved tool for drug efflux studies. *J Pharm Sci*. 2017;106(9):2909–2913. https://doi.org/10.1016/j.xphs.2017.04.018.
33. Brück S, Strohmeier J, Busch D, Drozdzik M, Oswald S. Caco-2 cells - expression, regulation and function of drug transporters compared with human jejunal tissue. *Biopharm Drug Dispos*. 2017;38(2):115–126. https://doi.org/10.1002/bdd.2025.
34. Irvine JD, Takahashi L, Lockhart K, et al. MDCK (Madin-Darby Canine Kidney) cells: a tool for membrane permeability screening. *J Pharm Sci*. 1999;88(1):28–33. https://doi.org/10.1021/js9803205.
35. Hanke U, May K, Rozehnal V, Nagel S, Siegmund W, Weitschies W. Commonly used nonionic surfactants interact differently with the human efflux transporters ABCB1 (p-glycoprotein) and ABCC2 (MRP2). *Eur J Pharm Biopharm*. 2010;76(2):260–268. https://doi.org/10.1016/j.ejpb.2010.06.008.
36. Bunchongprasert K, Shao J. Cytotoxicity and permeability enhancement of Capmul®MCM in nanoemulsion formulation. *Int J Pharm*. 2019;561:289–295. https://doi.org/10.1016/j.ijpharm.2019.03.010.
37. Li X, Sun J, Guo Z, Zhong D, Chen X. Carboxylesterase 2 and intestine transporters contribute to the low bioavailability of Allisartan, a prodrug of Exp3174 for hypertension treatment in humans. *Drug Metab Dispos*. 2019;47(8):843–853. https://doi.org/10.1124/dmd.118.085092.
38. Imai T, Imoto M, Sakamoto H, Hashimoto M. Identification of esterases expressed in Caco-2 cells and effects of their hydrolyzing activity in predicting human intestinal absorption. *Drug Metab Dispos*. 2005;33(8):1185–1190. https://doi.org/10.1124/dmd.105.004226.
39. Ölander M, Wiśniewski JR, Matsson P, Lundquist P, Artursson P. The proteome of filter-grown Caco-2 cells with a focus on proteins involved in drug disposition. *J Pharm Sci*. 2016;105(2):817–827. https://doi.org/10.1016/j.xphs.2015.10.030.
40. Hosokawa M. Structure and catalytic properties of carboxylesterase isozymes involved in metabolic activation of prodrugs. *Molecules*. 2008;13(2):412–431. https://doi.org/10.3390/molecules13020412.
41. Wang D, Zou L, Jin Q, Hou J, Ge G, Yang L. Human carboxylesterases: a comprehensive review. *Acta Pharm Sin B*. 2018;8(5):699–712. https://doi.org/10.1016/j.apsb.2018.05.005.
42. Fleming CD, Bencharit S, Edwards CC, et al. Structural insights into drug processing by human carboxylesterase 1: tamoxifen, mevastatin, and inhibition by Benzil. *J Mol Biol*. 2005;352(1):165–177. https://doi.org/10.1016/j.jmb.2005.07.016.
43. Kubackova J, Holas O, Zbytovska J, et al. Oligonucleotide delivery across the Caco-2 monolayer: the design and evaluation of self-emulsifying drug delivery systems (SEDDS). Pharmaceutics. 2021;13(4):459. https://doi.org/10.3390/pharmaceutics13040459.
44. Li J, Li L-B, Nessah N, et al. Simultaneous analysis of dissolution and permeation profiles of nanosized and microsized formulations of indomethacin using the in

vitro dissolution absorption system 2. *J Pharm Sci*. 2019;108(7):2334–2340. https://doi.org/10.1016/j.xphs.2019.01.032.
45. Hofmann AF, Borgström B. The intraluminal phase of fat digestion in man: the lipid content of the micellar and oil phases of intestinal content obtained during fat digestion and absorption*. *J Clin Invest*. 1964;43(2):247–257. https://doi.org/10.1172/JCI104909.
46. Liddle RA, Goldfine ID, Rosen MS, Taplitz RA, Williams JA. Cholecystokinin bioactivity in human plasma. Molecular forms, responses to feeding, and relationship to gallbladder contraction. *J Clin Invest*. 1985;75(4):1144–1152. https://doi.org/10.1172/JCI111809.
47. Williams HD, Anby MU, Sassene P, et al. Toward the establishment of standardized *in Vitro* tests for lipid-based formulations. 2. the effect of bile salt concentration and drug loading on the performance of Type I, II, IIIA, IIIB, and IV formulations during *in Vitro* digestion. *Mol Pharm*. 2012;9(11):3286–3300. https://doi.org/10.1021/mp300331z.
48. Wang TY, Liu M, Portincasa P, Wang DQ-H. New insights into the molecular mechanism of intestinal fatty acid absorption. *Eur J Clin Invest*. 2013;43(11):1203–1223. https://doi.org/10.1111/eci.12161.
49. Mu H. The digestion of dietary triacylglycerols. *Prog Lipid Res*. 2004;43(2):105–133. https://doi.org/10.1016/S0163-7827(03)00050-X.
50. Nauli AM, Sun Y, Whittimore JD, Atyia S, Krishnaswamy G, Nauli SM. Chylomicrons produced by Caco-2 cells contained ApoB-48 with diameter of 80-200nm. *Physiol Rep*. 2014;2(6):e12018. https://doi.org/10.14814/phy2.12018.
51. Levy E, Yotov W, Seidman EG, Garofalo C, Delvin E, Ménard D. Caco-2 cells and human fetal colon: a comparative analysis of their lipid transport. Biochim Biophys Acta. 1999;1439(3):353–362. https://doi.org/10.1016/S1388-1981(99)00085-2.